Targeted Imaging of EGF Receptor Expression in Gli36 Tumor Xenografts Using Monoclonal Antibody Conjugates

M. S. Shazeeb[1,2], C. H. Sotak[1,3], and A. Bogdanov[3]

[1]Department of Biomedical Engineering, Worcester Polytechnic Institute, Worcester, MA, United States, [2]Graduate School of Biomedical Sciences, University of Massachusetts Medical School, Worcester, MA, United States, [3]Department of Radiology, University of Massachusetts Medical School, Worcester, MA, United States

Introduction: Overexpression of wtEGFR (170kD epidermal growth factor receptor) due to gene amplification is implicated in the development of aggressive gliomas. Receptor imaging *in vivo* could potentially provide more accurate tumor detection, typing, and staging. The goal of this study was to image EGFR-overexpressing orthotopic human glioma tumors using local retention of a paramagnetic molecular substrate di(tyramido)-DTPA(Gd) (diTyr-DTPA(Gd), Fig. 1A) as a strategy of targeted MR signal enhancement. EGF receptor was targeted by using monoclonal antibody (humanized mAb EMD72000, Merck KGaA) conjugates with peroxidase (HRP) and glucose oxidase (GO) as a self-complementing enzymatic signal amplification system (Bogdanov et al. 2007). The substrate (hydrogen peroxide) for the key enzymatic reaction, catalyzed by a HRP conjugate was generated by a conjugate of mAb with glucose oxidase (GO) as depicted in Fig. 1B. MR signal was generated at the EGFR expression sites due to a binding of reactive intermediate products of diTyr-DTPA(Gd) oxidation by HRP.

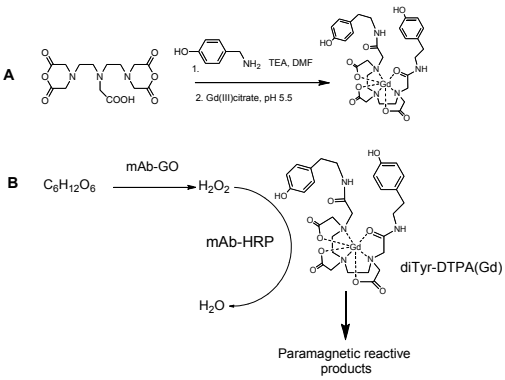

Fig. 1 A – Chemical synthesis diTyr-DTPA(Gd); **B** – Reaction of peroxidase substrate diTyr-DTPA(Gd) with the enzyme pair (glucose oxidase/peroxidase) conjugated to anti-EGFR mAb.

Methods: Paramagnetic substrate diTyr-DTPA(Gd) was synthesized as shown in Fig. 1A (Querol et al. 2007). MAb conjugates were synthesized by linking HRP or GO to mAB via bisaromatic hydrazone bonds. Size-exclusion HPLC purified conjugates were characterized in human glioma Gli36 cell culture and the ratios of HRP and GO conjugates were selected to provide the maximum signal at the lowest toxicity. Gli36ΔEGFR tumor xenografts were stereotaxically implanted in the brains of athymic rats. MR images were acquired in a Philips Achieva 3.0T/60 cm equipped with 80mT/m actively shielded gradients. T1-weighted (T1wt) spin-echo (SE) MRI was performed with the following parameters: TR/TE = 700ms/8.2ms, FOV = 2.56 cm X 2.56 cm, matrix = 256x128, NEX = 4. Two weeks after tumor implantation, each animal was anesthetized with isofluorane and imaged on two occasions. 1) Day 1 – a pre-contrast image was acquired followed by IV injection of 0.1 mmol/kg diTyr-DTPA(Gd). Twenty T1wt images were then acquired over a 2-h period. 2) Day 2 – targeted mAb conjugates (100 μg mAb/animal) were injected IV. Three hours later, a pre-contrast image was acquired followed by IV injection of 0.1 mmol/kg diTyr-DTPA(Gd). Thirty T1wt images were then acquired over a 3-h period. Pre-contrast T2wt SE images were acquired on both days to corroborate the presence of tumor observed in the T1wt slices. Animals were sacrificed and the frozen brain sections were stained for peroxidase activity and EGFR expression.

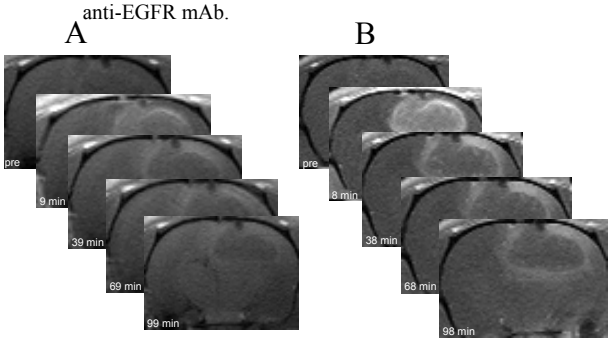

Fig. 2 – Sequential T1wt rat brain images showing Gli36 tumor xenografts. **A)** Day 1 – after IV injection of diTyr-DTPA(Gd) with no conjugates. **B)** Day 2 – after IV injection of di-(tyramido)-DTPA (Gd) with conjugates in the same animal.

Results and Discussion: T1wt images showed strong initial enhancement of the tumor within minutes after IV contrast injection – either with (Day 2) or without (Day 1) the preinjection of mAb conjugates (Fig. 2). However, the initial enhancement of the tumor following IV injection of diTyr-DTPA(Gd) with the conjugates (Fig 2B – 8 min) was significantly higher than that on Day 1 in the same animal (Fig. 2A – 9 min). Furthermore, contrast agent retention was higher on Day 2 (Fig. 2B) – as compared to Day 1 (Fig. 2A) – particularly in the tumor rim region over the same time period. Spatial deconvolution of the tumor signal showed different rates of contrast agent washout for the rim and the core regions. Bioelimination of diTyr-DTPA(Gd) was quantified by fitting the temporal signal-intensity decay for each tumor region. For Day 1, a monoexponential [Eq. 1] best modeled the data. For Day 2, a biexponential [Eq. 2] was a more appropriate model.

$$y_{mono} = A_0 \cdot e^{-t/\tau_0} + offset \qquad \text{[Eq. 1]}$$

$$y_{bi} = A_1 \cdot e^{-t/\tau_1} + A_2 \cdot e^{-t/\tau_2} \qquad \text{[Eq. 2]}$$

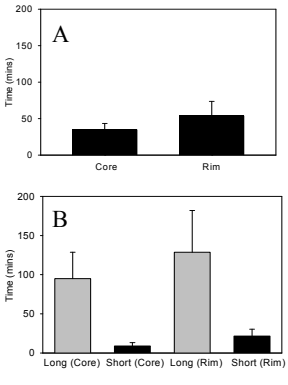

Fig. 3 – **A)** Day 1 – washout time constants τ_0 for diTyr-DTPA(Gd) in the absence of conjugates in tumor rim and core regions (n=8). **B)** Day 2 – long τ_1 and short τ_2 washout time constants for diTyr-DTPA(Gd) in the presence of conjugates in tumor rim and core regions (n=4).

For the contrast agent without conjugates (Day 1), the washout time constant (τ_0) for the rim (54±20 ms) was significantly higher ($P < 0.02$) than that of the core region (35±9 ms) (Fig. 3A). This difference was attributed to the higher vascular density in the periphery of the tumor. For the Day 1 data, the single component – with time constant τ_0 – was attributed to unbound contrast agent. For the contrast agent with conjugates (Day 2), the biexponential model yielded a long and a short signal-decay time constant (τ_1 and τ_2, respectively) for both the tumor rim and core regions (Fig. 3B). The component with the short time constant (τ_2) was attributed to unbound contrast agent while the component with the long time constant (τ_1) was attributed to contrast agent bound to the conjugate. The time constant associated with the bound contrast agent (τ_1) was not significantly different between the rim and the core regions. However, for the component associated with the unbound contrast agent, the time constant (τ_2) for the rim (22±9 ms) was significantly higher ($P < 0.03$) than that of the core region (9±4 ms) (Fig. 3B). Furthermore, for the Day 2 data, the time constants associated with the unbound contrast agent (τ_2) in the tumor rim and core regions were significantly less than the corresponding washout time constants (τ_0) in the same regions on Day 1 (22±9 ms vs. 54±20 ms in the rim ($P < 0.002$); 9±4 ms vs. 35±9 ms in the core ($P < 0.00003$), respectively). Although the contrast agent is considered to be unbound in each case, the reduced washout times on Day 2 may arise from a decrease in vascular permeability due to the perivascular accumulation of high-affinity antibody-conjugates (Thurber et al. 2008) and associated cytotoxicity. The presence of extravasated and bound conjugates in tumor tissue was proven by using anti-HRP and anti-GO histochemical staining of the frozen brain sections.

Conclusions: Following conjugate administration (Day 2), the increase in contrast agent retention was attributed to a second contrast-agent component (with the long time constant, τ_1) that was not present when diTyr-DTPA(Gd) alone was administered (Day 1). This long-retained component is consistent with enzyme-mediated coupling of the paramagnetic agent to EGFR-overexpressing cells in the tumor; allowing effective MRI visualization of conjugate co-localization at the targeted site.

References: Bogdanov, A., et al. (2007). Bioconjug Chem **18**: 1123-30. Querol, M., et al. (2007). Chembiochem **8**: 1637-41. Thurber, GM, et al. (2008). Adv Drug Del Revs **60**: 1421-1434.